Check for updates

# Photoelectron spectroscopy and density functional theory studies of (fructose + (H$_2$O)$_n$)$^−$ (n = 1–5) anionic clusters†

Zhen Zeng and Elliot R. Bernstein [iD] *

Photoelectron spectroscopy (PES) and density functional theory (DFT) based calculations are executed to characterize gas phase, isolated (fructose + (H$_2$O)$_n$)$^−$ (n = 1–5) anionic species produced using a matrix assisted laser desorption ionization (MALDI) method. Gas phase, isolated (fructose + (H$_2$O)$_n$)$^−$ (n = 1–5) cluster anions mainly exist as open chain structures with conformational and positional isomers in the present experiments. Some cyclic structures of (fructose + (H$_2$O)$_n$)$^−$ (n = 3, 4) are apparently present in the experiments and their VDEs can contribute to the lower energy shoulders of PES features observed for (fructose + (H$_2$O)$_n$)$^−$ (n = 3, 4). Cyclic (fructose + (H$_2$O)$_n$)$^−$ (n = 1–5) clusters have the added electron as dipole bound, whereas open chain structures have the added electron in a valence orbital. Water molecules in open chain anions predominantly interact with the (1)C side (including (1)OH, (2)O, and (3)OH) of fructose$^−$: they finally form a quasi-cubic structure with OH groups and carbonyl O in the most stable structures for (fructose + (H$_2$O)$_4$)$^−$ and (fructose + (H$_2$O)$_5$)$^−$ cluster anions. Water molecules solvating cyclic anions form water–water hydrogen bond networks that preferentially interact with OH groups at the (1), (2), and (3) positions of fructose pyranose anions, and the (3), (4), and (6) positions of fructose furanose anions. Structures of neutral (fructose + (H$_2$O)$_n$) (n = 1–5) have pyranose structures as the lower energy isomers rather than open chain structures: this observation is consistent with the fructose solution tautomeric equilibrium with neutral fructose pyranose being the preponderant species. Water molecules also tend to form water–water hydrogen bond networks, interacting with OH groups at (1), (2), and (3) positions for neutral pyranose conformations.
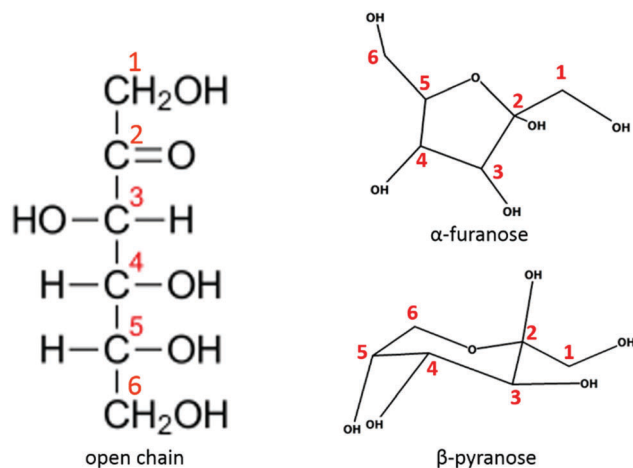
## I. Introduction

Solvation of carbohydrates is a fundamental biochemical and physicochemical process occurring within living systems. Carbohydrate (saccharide) solutions are additionally of significant importance in both the food and pharmaceutical industries. Biological, physical, and chemical properties of carbohydrates in solution are strongly correlated with the relative concentrations of different tautomeric forms, as well as with the balance between solute–solvent interactions, solute–solute interactions, and solvent–solvent interactions. Understanding the solvation process helps in the elucidation of the biological functions of carbohydrates, *e.g.*, molecular recognition and biological catalysis. Some research results even suggest that water in carbohydrate solutions can not only act as a solvent, but can also act

as an active and essential participant during carbohydrate molecular recognition processes.[1–4]

The solubility and hydration number of saccharides depend on individual saccharide intrinsic molecular structures. Solute–solvent interactions in aqueous solutions of saccharides also lead to configurational and conformational equilibria of different tautomeric isomers. Fructose (Scheme 1) has been shown to exist in at least five equilibrating tautomers in solutions (α- and β-pyranose, α- and β-furanose and an open chain ketose form): at equilibrium in water at *ca.* 300 K, β-D-fructopyranose is the preponderant isomer, followed by β-D-fructofuranose, and then α-D-fructofuranose.[5–7] Some small amounts of these components can be present in an open chain keto form or as α-D-fructopyranose.[6,8,9] Hydrogen bonds, including intermolecular and intramolecular ones, are the major cooperative interactions in the hydrated sugar system. Conformational preferences of most carbohydrates evidence structures for which cooperative effects enhance the stability of the conformation to which water molecules bind.[10] These solute–solvent interactions also influence bulk water structures (as can be expected for entropically driven reactions). Fructose can disrupt the water structure at

*Department of Chemistry, NSF ERC for Extreme Ultraviolet Science and Technology, Colorado State University, Fort Collins, CO 80523, USA. E-mail: erb@colostate.edu*

This journal is © the Owner Societies 2017

*Phys. Chem. Chem. Phys.*, 2017, **19**, 31121–31137 | 31121

**Scheme 1** Structures of D-fructose with C atom numbering.

low concentrations, while at high concentrations fructose can enhance the water structure.[11,12]

A number of experimental techniques (including infrared absorption,[13] Raman scattering,[14,15] THz time-domain attenuated total reflection (THz TD-ATR),[16] nuclear magnetic resonance (NMR),[17] neutron scattering,[18] viscosity measurements,[19] and dielectric[20] spectroscopy), as well as molecular dynamic computer simulations,[21–24] have been undertaken to characterize the hydration extent of saccharide and/or water hydrogen bond disruption in aqueous saccharide solutions. Unfortunately, the different experimental techniques employed have different hydration state criteria and definitions, which can yield unclear and inconsistent identification of carbohydrate hydration characteristics. Fructose hydrates have been investigated by IR spectroscopy and fructose penta- and mono-hydrates are identified in D-fructose aqueous solutions throughout the concentration range from nearly pure water to the fructose saturation limit.[13] THz TD-ATR measurements reveal that the determined hydration number is highly correlated with the number of equatorial hydroxyl groups of saccharides and is inversely dependent on solute concentration.[16] Exact structural investigations need to be explored to understand the hydration mechanism as well as the solute–solvent interactions. Studies of gas phase, isolated hydrated fructose clusters can provide a clear potential surface map for interactions between fructose and water, as well as the intrinsic conformations of the saccharide itself, in the absence of environmental or substitute effects.

Investigation of saccharide–water interactions can also shed light on interpreting the sweetness of sugars. The sweet taste sensation of saccharides comes from intermolecular hydrogen bonding (AH–B unit glycophore) between the sweetener and the sweet receptor. The degree of perceived sweetness depends on the strength of the two hydrogen bonds formed.[25,26] The third component of sweetness, called "γ", is comprised of a hydrophobic center in the sweetener with the sweetness triangle formation.[27–30] The molecular theory of sweet taste is still evolving: for instance, a multipoint attachment theory has been proposed. This suggests that the number of interaction sites in

a sweetener may be equal to or lower than eight.[31] Based on the investigations of sugar sweetness from the point of view of water–sugar interactions and the general sugar behavior in water, a link between the hydration shell of sugars and their degree of sweetness has also been proposed.[32,33]

The present study has been undertaken to elucidate microscopic hydration processes for, as well as hydration structures and properties of, fructose. Anion photoelectron spectroscopic experiments and DFT calculations are conducted on gas phase, isolated (fructose + $(H_2O)_n)^-$ ($n = 1–5$) anionic cluster species in order to investigate their electronic and geometric structures. The anionic structures (conformational and positional) of (fructose + $(H_2O)_n)^-$ that exist in the present experiments are assigned based on the agreement between calculated and observed VDEs. Conformational isomers (open chain, furanose, pyranose,...) have different geometries, but the same positions for added $H_2O$ moieties. Positional isomers have different added $H_2O$ moiety positions, but have similar conformations. Based on the experimentally validated calculation algorithm, the corresponding neutral structures are also identified.

## II. Experimental procedures

The experimental apparatus consists of three parts: a pulsed supersonic nozzle with an attached matrix assisted laser desorption ionization (MALDI) source, a reflectron time of flight mass spectrometer (RTOFMS), and a magnetic bottle photoelectron TOF spectrometer (MBTOFPES). Details of this system (RTOFMS/MBTOFPES) can be found in our previous publications.[34,35] The nozzle employed for the sample beam generation is constructed from a Jordan Co. pulsed valve and a laser desorption attachment. All sample drums for the MALDI are prepared by wrapping a Zn substrate on a clean Al drum.[36] A mixed solution of D-fructose and matrix (DCM) dye with a mole ratio ~3:2 in a solvent (typically, methanol or acetonitrile) is uniformly sprayed on the drum/substrate surface using an air atomizing spray nozzle (Spraying System Co.) with a siphon pressure of 10 psig. During the spraying process, the sample drum is rotated under heat of a halogen lamp in a fume hood to ensure deposition of D-fructose and the matrix on the drum surface is homogeneous and dry. The well-coated and dried sample drum is then placed in the laser ablation head/nozzle assembly and put into the vacuum chamber. Second harmonic (532 nm) light pulses from a Nd:YAG laser are used to ablate the sample drum, which rotates and translates simultaneously to maintain a fresh sample area for each laser ablation pulse. Whole D-fructose molecules are desorbed from the drum, interact with other species (including electrons) in the ablated material plume, entrained in the supersonic flow of helium carrier gas seeded with water vapor with a 50 psi backing pressure through a $2 \times 60$ mm channel in the ablation head, and expanded into the sample chamber. With a closed pulsed valve, the RTOFMS chamber pressure is $\sim 6 \times 10^{-8}$ Torr. The generated molecular anions are pulsed into the RTOFMS and are mass analyzed using the RTOFMS. For PES experiments, specific anions are first mass selected and

31122 | *Phys. Chem. Chem. Phys.*, 2017, **19**, 31121–31137

This journal is © the Owner Societies 2017

decelerated before interacting with a 355 nm (3.496 eV), or 266 nm (4.661 eV) laser beam from another Nd:YAG laser in the photodetachment region. Photodetached electrons are collected and energy analyzed using a MBTOFPES at nearly 100% efficiency. The photodetachment laser is operated at a 10 Hz repetition rate, while the ablation laser is synchronously triggered at 5 Hz. Data are collected at 5 Hz employing a background subtraction with alternation of the ablation laser on/off if the detachment laser generates 266 nm or higher energy photons. Every photoelectron spectrum is calibrated by the known spectra of $Cu^-$ at the employed detachment photon energy. The photoelectron energy resolution is ~4% (40 meV for 1 eV kinetic energy electrons), as anticipated for a 1 m PES flight tube.

## III. Computational methods

DFT (B3LYP and M062X functionals) methods with a 6-311++G(d,p) basis set are validated to be efficient and accurate for electronic and geometric property calculations of gas phase sugar molecular anions and neutrals based on fructose and ribose in recently reported studies.[37,38] In the present work, all calculations are executed using density function theory (DFT) employing Becke's three-parameter hybrid (B3LYP)[39–41] functional and a 6-311++G(d,p) or 6-31++G(d) basis set for all atoms, as implemented in the Gaussian 09 program.[42] The low energy isomers for every species are reoptimized employing a M062X[43,44] functional with the same basis set. No symmetry restrictions are applied for the calculations. Optimization of the low lying isomers for each anion and neutral are performed with harmonic vibrational frequencies calculated to confirm that the obtained structures are the true local minima. Theoretical VDEs for each anionic species are calculated as the energy difference between the ground state of the anion and its corresponding neutral at the same structure as the anion. For a further electronic structure based understanding of the observed $(fructose + (H_2O)_n)^-$ ($n = 1$–5) species behavior, a Natural Bond Orbital (NBO, also from the Gaussian 09 program) analysis is performed based on the B3LYP functional and the 6-311++G(d,p) or 6-31++G(d) basis set.

## IV. Experimental results

Through our MALDI processes, $(fructose + (H_2O)_n)^-$ ($n = 1$–5) anionic clusters are observed in the mass spectrum, as shown in Fig. 1. The photoelectron spectra of $(fructose + (H_2O)_n)^-$ ($n = 0$–5) recorded with 355 nm photons are presented in Fig. 2. VDEs are measured from the maxima of the corresponding PES peaks. The VDEs of $(fructose + (H_2O)_n)^-$ ($n = 1$–5) clusters are summarized in Tables 1 and 2. The photoelectron spectrum of $fructose^-$ shows two components, centered at 1.93 and 1.58 eV, which can be assigned to three different conformational isomers, as reported before.[37] The photoelectron spectrum of $(fructose + H_2O)^-$ displays narrower features compared to those of the bare ion. It exhibits the major peak centered at 1.58 eV and a small one at 1.99 eV, as well as a long tail to above 2 eV. The photoelectron
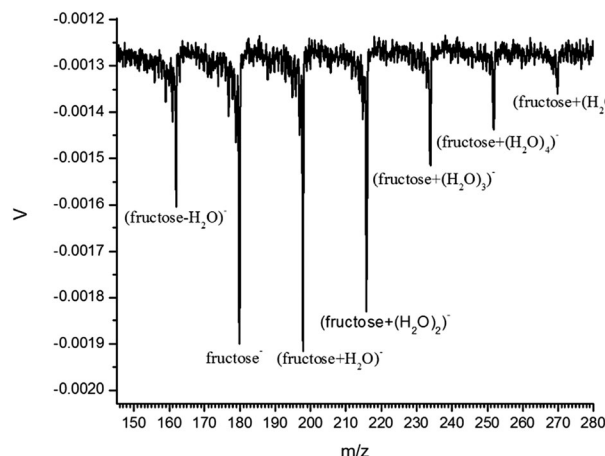


Fig. 1 Mass spectrum of fructose with sample (D-fructose/DCM) sprayed on a Zn surface.



Fig. 2 Photoelectron spectra of $(fructose + (H_2O)_n)^-$ ($n = 0$–5) recorded with 355 nm photons with sample (D-fructose/DCM) spayed on a Zn surface.

spectra of $(fructose + (H_2O)_n)^-$ ($n = 2$–5) all display broad features with slightly and gradually increasing electron binding energy (EBE). The PES feature of $(fructose + (H_2O)_2)^-$ is centered from ~1.97 eV to above 3 eV. The photoelectron spectra of $(fructose + (H_2O)_3)^-$ and $(fructose + (H_2O)_4)^-$ show broad peaks centered at ~2.18 eV and 2.25 eV, respectively, to above 3 eV.

**Table 1** Relative energies ($\Delta E$) of the low energy isomers of (fructose + $(H_2O)_n$)$^-$ ($n = 1–2$), and comparison of their calculated VDEs based on B3LYP/6-311++G(d,p) and M062X/6-311++G(d,p) algorithms. Experimental VDE values are given in the right hand column. All energies are in eV. Cluster anions with VDEs *ca.* 1 eV or lower typically have the added electron as dipole bound (see Fig. 10)

| | | B3LYP/6-311++G(d,p) | | M062X/6-311++G(d,p) | | |
| --- | --- | --- | --- | --- | --- | --- |
| | | $\Delta E$ | Theo. VDE | $\Delta E$ | Theo. VDE | Exp. VDE |
| Fructose + $H_2O^-$ | Fructose + $H_2O^-$ (A) | 0.00 | 2.24 | 0.00 | 2.24 | |
| | Fructose + $H_2O^-$ (B) | 0.06 | 2.36 | 0.06 | 2.33 | |
| | Fructose + $H_2O^-$ (C) | 0.13 | 2.17 | 0.17 | 2.16 | |
| | Fructose + $H_2O^-$ (D) | 0.24 | 1.99 | 0.19 | 2.30 | 1.99 |
| | Fructose + $H_2O^-$ (E) | 0.34 | 1.98 | 0.39 | 1.90 | |
| | Fructose + $H_2O^-$ (F) | 0.34 | 1.86 | 0.42 | 1.82 | |
| | Fructose + $H_2O^-$ (G) | 0.44 | 1.76 | 0.48 | 1.70 | 1.58 |
| | Fructose + $H_2O^-$ (H) | 0.45 | 1.83 | 0.48 | 1.77 | |
| | Fructose + $H_2O^-$ (I) | 0.55 | 1.76 | 0.61 | 1.70 | |
| | Fructose + $H_2O^-$ (J) | 0.79 | 0.40 | 0.53 | 0.20 | |
| | Fructose + $H_2O^-$ (K) | 0.92 | 0.47 | 0.76 | 0.36 | |
| (Fructose + $(H_2O)_2$)$^-$ | (Fructose + $(H_2O)_2$)$^-$ (A) | 0.00 | 2.76 | 0.08 | 2.56 | ~1.97 to ~3 |
| | (Fructose + $(H_2O)_2$)$^-$ (B) | 0.01 | 2.54 | 0.00 | 2.40 | |
| | (Fructose + $(H_2O)_2$)$^-$ (C) | 0.02 | 2.14 | 0.03 | 2.22 | |
| | (Fructose + $(H_2O)_2$)$^-$ (D) | 0.02 | 2.59 | 0.13 | 2.62 | |
| | (Fructose + $(H_2O)_2$)$^-$ (E) | 0.08 | 2.36 | 0.07 | 2.28 | |
| | (Fructose + $(H_2O)_2$)$^-$ (F) | 0.19 | 2.47 | 0.23 | 2.50 | |
| | (Fructose + $(H_2O)_2$)$^-$ (G) | 0.24 | 2.42 | 0.14 | 2.53 | |
| | (Fructose + $(H_2O)_2$)$^-$ (H) | 0.32 | 1.97 | 0.37 | 2.22 | |
| | (Fructose + $(H_2O)_2$)$^-$ (I) | 0.33 | 2.27 | 0.37 | 2.18 | |
| | (Fructose + $(H_2O)_2$)$^-$ (J) | 0.35 | 2.24 | 0.40 | 2.16 | |
| | (Fructose + $(H_2O)_2$)$^-$ (K) | 0.36 | 2.12 | 0.41 | 2.04 | |
| | (Fructose + $(H_2O)_2$)$^-$ (L) | 0.38 | 1.80 | 0.46 | 1.84 | |
| | (Fructose + $(H_2O)_2$)$^-$ (M) | 0.42 | 2.10 | 0.33 | 2.18 | |
| | (Fructose + $(H_2O)_2$)$^-$ (N) | 0.79 | 0.61 | 0.56 | 0.60 | |
| | (Fructose + $(H_2O)_2$)$^-$ (O) | 0.97 | 0.77 | 0.86 | 0.76 | |

Shoulders in the range from 0.5 eV to 1.5 eV before the major features of (fructose + $(H_2O)_3$)$^-$ and (fructose + $(H_2O)_4$)$^-$, appear as well. The photoelectron spectrum of (fructose + $(H_2O)_5$)$^-$ has a broad feature centered from ~2.88 to above ~3.3 eV.

## V.   Theoretical results

The low energy isomers of (fructose + $(H_2O)_n$)$^{-/0}$ ($n = 1–2$) are first optimized at the B3LYP/6-311++G(d,p) level of theory, and those of (fructose + $(H_2O)_n$)$^{-/0}$ ($n = 3–5$) are first optimized at the B3LYP/6-311++G(d) level of theory. The lower lying isomers of (fructose + $(H_2O)_n$)$^-$ ($n = 1–5$) are then reoptimized *via* the M062X/6-311++G(d,p) or M062X/6-31++G(d) approach, based on the initial B3LYP structures. From these two approaches, we can obtain similar calculated VDEs of every specific isomer for each cluster, which are in good agreement with the experiments, as shown in Tables 1 and 2, and nearly identical geometrical structures, as can be seen in Fig. 4, 6–9 and Fig. S16–S20 (ESI†). Different conformation energy orderings ($\Delta E_s$) arise for calculations employing different DFT functionals for such flexible polymorphic species with nearly degenerate energy isomers residing on a flat potential energy surface.

The low lying isomers of (fructose + $(H_2O)_n$)$^-$ ($n = 1–5$) anions, as well as their corresponding neutrals, are summarized in Fig. 4–9 and Fig. S11–S15 (ESI†). More isomers are presented in the ESI.† Note that the figure numbers in the ESI† document are related to those of the text figures, for example Fig. 4 ⇔ Fig. S4 (ESI†). Calculated VDEs and relative energies

of their anions are summarized and compared with the experimental results in Tables 1 and 2.

For geometrical optimization of (fructose + $(H_2O)_n$)$^-$ ($n = 1–5$), three conformational open chain isomers (A), (B), (C) and the lowest energy pyranose (D) and furanose (E) structures of fructose$^-$ (see Fig. 3) are chosen to be the initial structures followed by adding $H_2O$ moieties at different possible positions. The bigger clusters can evolve from smaller clusters by adding more $H_2O$ moieties systematically at different possible positions. Recall that isomer fructose$^-$ (A) contributes to the higher EBE component (1.93 eV) of the photoelectron spectrum, while fructose$^-$ isomers (B) and (C) contribute to the lower EBE part (1.58 eV).[37]

### a.   (Fructose + $H_2O$)$^-$

Typical low lying isomers of (fructose + $H_2O$)$^-$ are displayed in Fig. 4. More isomers can be seen in the ESI.† Isomer (A) is developed from open chain fructose$^-$ (A) with the first $H_2O$ moiety interacting with the OH group at (1) position and carbonyl O at (2) position. Its calculated VDE is 2.24 eV, in accord with the long tail range of the PES feature. Isomers (B) and (C) also arise from fructose$^-$ (A) with the $H_2O$ molecule binding to the carbonyl O and (3)OH group, respectively. Their VDEs are calculated to be 2.36 and 2.17 eV, respectively, also belonging to the tail region of the spectral feature. (Fructose + $H_2O$)$^-$ isomer (D) from fructose$^-$ (A) has the added $H_2O$ moiety bound through (4)OH and (6)OH groups. This (fructose + $H_2O$)$^-$ isomer has a theoretical VDE of 1.99 eV, in good agreement with a small peak centered at 1.99 eV.

**Table 2** Relative energies ($\Delta E$) of the low energy isomers of (fructose + $(H_2O)_n)^-$ ($n$ = 3–5), and comparison of their calculated VDEs based on B3LYP/6-31++G(d) and M062X/6-31++G(d) algorithms. Experimental VDE values are given in the right hand column. All energies are in eV. Cluster anions with VDEs *ca.* 1 eV or lower typically have the added electron as dipole bound (see Fig. 10)

| | | B3LYP/6-31++G(d) | | M062X/6-31++G(d) | | |
| --- | --- | --- | --- | --- | --- | --- |
| | | $\Delta E$ | Theo. VDE | $\Delta E$ | Theo. VDE | Exp. VDE |
| (Fructose + $(H_2O)_3)^-$ | (Fructose + $(H_2O)_3)^-$ (A) | 0.00 | 2.64 | 0.00 | 2.61 | ∼2.18 to ∼3 |
| | (Fructose + $(H_2O)_3)^-$ (B) | 0.05 | 2.39 | 0.03 | 2.50 | |
| | (Fructose + $(H_2O)_3)^-$ (C) | 0.08 | 3.00 | 0.21 | 2.76 | |
| | (Fructose + $(H_2O)_3)^-$ (D) | 0.09 | 2.86 | 0.05 | 2.67 | |
| | (Fructose + $(H_2O)_3)^-$ (E) | 0.11 | 2.75 | 0.04 | 2.57 | |
| | (Fructose + $(H_2O)_3)^-$ (F) | 0.13 | 2.41 | 0.12 | 2.41 | |
| | (Fructose + $(H_2O)_3)^-$ (G) | 0.17 | 3.08 | 0.22 | 3.00 | |
| | (Fructose + $(H_2O)_3)^-$ (H) | 0.21 | 2.84 | 0.08 | 2.76 | |
| | (Fructose + $(H_2O)_3)^-$ (I) | 0.26 | 2.78 | 0.23 | 2.76 | |
| | (Fructose + $(H_2O)_3)^-$ (J) | 0.32 | 2.40 | 0.25 | 2.39 | |
| | (Fructose + $(H_2O)_3)^-$ (K) | 0.36 | 2.40 | 0.43 | 2.38 | |
| | (Fructose + $(H_2O)_3)^-$ (L) | 0.37 | 2.51 | 0.38 | 2.49 | |
| | (Fructose + $(H_2O)_3)^-$ (M) | 0.39 | 2.51 | 0.36 | 2.44 | |
| | (Fructose + $(H_2O)_3)^-$ (N) | 0.73 | 0.87 | 0.47 | 0.71 | 1.00 |
| | (Fructose + $(H_2O)_3)^-$ (O) | 0.82 | 1.10 | 0.53 | 0.95 | |
| | (Fructose + $(H_2O)_3)^-$ (P) | 0.96 | 1.23 | 0.80 | 1.26 | |
| | (Fructose + $(H_2O)_3)^-$ (Q) | 0.97 | 0.98 | 0.84 | 0.85 | |
| (Fructose + $(H_2O)_4)^-$ | (Fructose + $(H_2O)_4)^-$ (A) | 0.00 | 2.88 | 0.00 | 2.89 | ∼2.25 to ∼3 |
| | (Fructose + $(H_2O)_4)^-$ (B) | 0.12 | 2.74 | 0.26 | 2.60 | |
| | (Fructose + $(H_2O)_4)^-$ (C) | 0.19 | 2.87 | 0.23 | 3.09 | |
| | (Fructose + $(H_2O)_4)^-$ (D) | 0.21 | 3.18 | 0.37 | 3.07 | |
| | (Fructose + $(H_2O)_4)^-$ (E) | 0.21 | 3.10 | 0.40 | 3.07 | |
| | (Fructose + $(H_2O)_4)^-$ (F) | 0.21 | 2.86 | 0.29 | 2.81 | |
| | (Fructose + $(H_2O)_4)^-$ (G) | 0.26 | 2.62 | 0.32 | 2.68 | |
| | (Fructose + $(H_2O)_4)^-$ (H) | 0.29 | 2.68 | 0.28 | 2.67 | |
| | (Fructose + $(H_2O)_4)^-$ (I) | 0.30 | 2.64 | 0.32 | 2.67 | |
| | (Fructose + $(H_2O)_4)^-$ (J) | 0.36 | 2.89 | 0.47 | 2.71 | |
| | (Fructose + $(H_2O)_4)^-$ (K) | 0.38 | 2.91 | 0.40 | 2.85 | |
| | (Fructose + $(H_2O)_4)^-$ (L) | 0.59 | 2.69 | 0.54 | 2.59 | |
| | (Fructose + $(H_2O)_4)^-$ (M) | 0.87 | 0.92 | 0.82 | 0.73 | |
| | (Fructose + $(H_2O)_4)^-$ (N) | 0.96 | 1.07 | 0.77 | 1.12 | |
| | (Fructose + $(H_2O)_4)^-$ (O) | 1.05 | 1.45 | 1.05 | 1.48 | |
| | (Fructose + $(H_2O)_4)^-$ (P) | 1.07 | 1.35 | 1.00 | 1.10 | |
| (Fructose + $(H_2O)_5)^-$ | (Fructose + $(H_2O)_5)^-$ (A) | 0.00 | 2.97 | 0.00 | 3.16 | ∼2.88 to ∼3.3 |
| | (Fructose + $(H_2O)_5)^-$ (B) | 0.06 | 3.09 | 0.14 | 3.12 | |
| | (Fructose + $(H_2O)_5)^-$ (C) | 0.08 | 3.22 | 0.08 | 3.20 | |
| | (Fructose + $(H_2O)_5)^-$ (D) | 0.10 | 3.12 | 0.06 | 3.13 | |
| | (Fructose + $(H_2O)_5)^-$ (E) | 0.10 | 3.14 | 0.09 | 3.14 | |
| | (Fructose + $(H_2O)_5)^-$ (F) | 0.15 | 2.77 | 0.39 | 2.64 | |
| | (Fructose + $(H_2O)_5)^-$ (G) | 0.15 | 3.16 | 0.32 | 3.08 | |
| | (Fructose + $(H_2O)_5)^-$ (H) | 0.32 | 2.98 | 0.48 | 2.95 | |
| | (Fructose + $(H_2O)_5)^-$ (I) | 0.34 | 2.91 | 0.29 | 2.77 | |
| | (Fructose + $(H_2O)_5)^-$ (J) | 0.34 | 2.85 | 0.44 | 2.89 | |
| | (Fructose + $(H_2O)_5)^-$ (K) | 0.44 | 3.14 | 0.47 | 3.09 | |
| | (Fructose + $(H_2O)_5)^-$ (L) | 0.65 | 2.94 | 0.64 | 2.81 | |
| | (Fructose + $(H_2O)_5)^-$ (M) | 0.95 | 1.09 | 0.91 | 0.82 | |
| | (Fructose + $(H_2O)_5)^-$ (N) | 0.96 | 1.08 | 0.83 | 1.12 | |
| | (Fructose + $(H_2O)_5)^-$ (O) | 0.98 | 1.38 | 1.05 | 1.21 | |
| | (Fructose + $(H_2O)_5)^-$ (P) | 1.04 | 1.43 | 1.06 | 1.48 | |

Both isomers (E) and (F) have the first water molecule interacting with (1)OH and (2)OH groups, but developed from fructose⁻ (B) and fructose⁻ (C), respectively. Their calculated VDEs are 1.98 and 1.86 eV, consistent with the experimental result (1.99 eV). Isomer (G) is evolved from fructose⁻ (C) by binding the H₂O moiety with (3)OH and (5)OH groups. Its theoretical VDE is 1.76 eV, close to the major peak of 1.58 eV. Both isomers (H) and (I) have a H₂O molecule bound to (5)OH and (6)OH groups, which come from fructose⁻ (C) and fructose⁻ (B), respectively. Their VDEs are calculated (1.83 and 1.76 eV)

which are close to the experimental feature (1.58 eV) too. Isomers (J) and (K) are cyclic structures with higher relative energies with respect to the most stable open chain isomer. The H₂O molecule interacts with the (1)OH and (3)OH groups of the pyranose structure, and with the (3)OH and (4)OH groups of the furanose geometry. They have calculated VDEs of 0.40 and 0.47 eV, very much lower than the experimental values. Overall, the photoelectron feature at 1.58 eV is mostly contributed by isomers (G), (H), and (I), while the small peak centered at 1.99 eV is related to isomers (D), (E) and (F). Isomers (A), (B) and (C) are also present
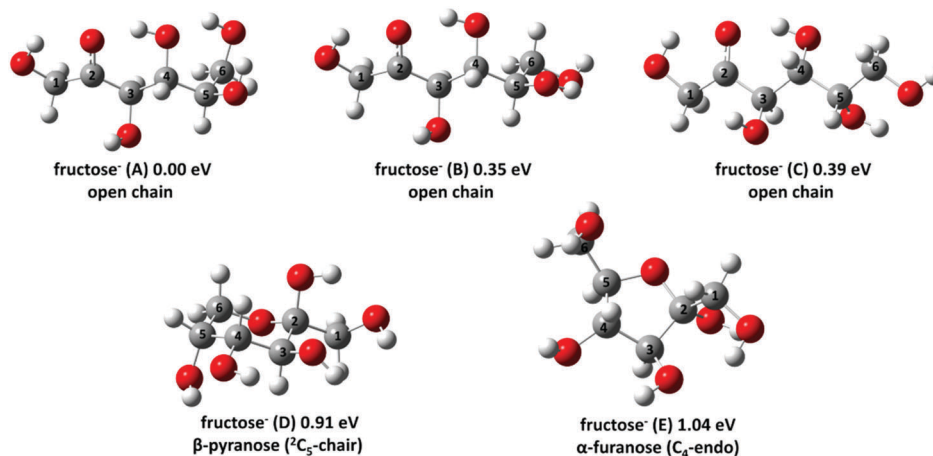
**Fig. 3** Optimized geometries of the typical low lying anionic isomers of fructose$^-$ based on B3LYP/6-311++G(d,p) calculations. The relative energies and structural polymorphs are indicated. C atom numberings are given. For open chain structures (1)C to (6)C is ordered from left to right. For both furanose and pyranose structures (1)C to (6)C is ordered from right to left in a clockwise direction. C atom numbering for open chain structures correspond to those in the cyclic structures, for instance (1)C ⇔ (1)C. Isomers (A), (B), and (C) are assigned to contribute to the PES feature of fructose: they exist in the gas phase according to our recent published results (see ref. 37). Isomers (D) and (E) are the lowest energy structures of anionic pyranose and furanose conformations, respectively.

in the experiments and contribute to the tail of PES features of (fructose + H$_2$O)$^-$. The neutral (fructose + H$_2$O) cluster, as shown in Fig. 5a, appears to have a pyranose structure as the global minimum isomer. The lowest energy furanose and open chain conformations are also given, with relative energies of 0.12 and 0.15 eV, respectively. The H$_2$O molecule binds with (2)OH and (3)OH in a pyranose structure, (1)OH and (3)OH in furanose, and (1)OH and (2)O in open chain conformations.

### b. (Fructose + (H$_2$O)$_2$)$^-$

The typical low lying anionic isomers of (fructose + (H$_2$O)$_2$)$^-$ are shown in Fig. 6. Similar to (fructose + H$_2$O)$^-$, open chain conformations comprise the lower energy isomers. The most stable isomer (A) can develop from (fructose + H$_2$O)$^-$ (A) by inserting the second H$_2$O molecule between the first one and (2)O. It has the calculated VDE of 2.76 eV, in the range of the broad PES feature (∼1.97 to above ∼3 eV) for (fructose + (H$_2$O)$_2$)$^-$. Isomer (B) can also evolve from (fructose + H$_2$O)$^-$ (A) by adding the second H$_2$O molecule at (2)O and forming a water–water hydrogen bond. Its calculated VDE of 2.54 eV is also in good agreement with the experimental values. Isomer (C) has the second H$_2$O molecule interacting with (1)OH and (3)OH groups with no water–water hydrogen bond formation. Its calculated VDE of 2.14 eV matches that observed experimentally. In isomer (D), the second H$_2$O molecule only forms a water–water hydrogen bond. Its VDE is calculated to be 2.59 eV, also in accord with experimental results. More isomers can develop from (fructose + H$_2$O)$^-$ by adding the second H$_2$O molecule at different positions, like (4)(5)(6), which also have comparable calculated VDEs to the experimental ones. Isomers (H) and (L) have similar positions for adding water moieties to isomer (C), but with conformational differences. Isomers (I) and (J) also have identical positions to those of isomer (B), but with conformational differences. They all have theoretical VDEs in good agreement with the

experimental determinations. Isomers (K) and (M) have relative energies of 0.36 and 0.42 eV, respectively. They can both evolve from isomer (fructose + H$_2$O)$^-$ (G) with the second H$_2$O molecule binding to (1)(2) and (4)(5) positions, respectively. They also evidence consistent theoretical VDEs with the experimental values. Isomers (N) and (O) are cyclic structures, developed from (fructose + H$_2$O)$^-$ (J) and (K), respectively. The second H$_2$O molecule binds with (3)OH and (4)OH groups in a pyranose structure, and inserts between the first water molecule and the (4)OH group in a furanose structure. Their theoretical VDEs are 0.61 and 0.77 eV, respectively, and they are both outside the experimental PES feature. More cyclic structures, with higher relative energies, are provided in the ESI.† Thus, many open chain structures coexist in the experiments to contribute to the broad PES feature of (fructose + (H$_2$O)$_2$)$^-$. The water moieties can interact with fructose$^-$ separately or form water dimer clusters to bind to fructose$^-$. As can be seen in Fig. 5b, the most stable structure of the neutral (fructose + (H$_2$O)$_2$) cluster is a pyranose isomer with the second H$_2$O molecule interacting with the first H$_2$O molecule as well as the (1)OH and (3)OH groups. The H$_2$O molecules in the open chain isomer form water–water hydrogen bonds and interact with fructose OH groups.

### c. (Fructose + (H$_2$O)$_3$)$^-$

Fig. 7 shows the low lying isomers of (fructose + (H$_2$O)$_3$)$^-$ developing from (fructose + (H$_2$O)$_2$)$^-$ by adding the third H$_2$O molecule at every possible position. Open chain conformations are still the energetically favored ones. Isomer (A) of (fructose + (H$_2$O)$_3$)$^-$ evolves from (fructose + (H$_2$O)$_2$)$^-$ (A) with the third H$_2$O molecule inserting between the (1)OH group and the adjacent water moiety. The calculated VDE is 2.64 eV, in the range (∼2.18 to above ∼3 eV) of the broad PES feature for (fructose + (H$_2$O)$_3$)$^-$. Isomer (B) has the third H$_2$O connecting the first and second water moieties of (fructose + (H$_2$O)$_2$)$^-$ (C) and forming two
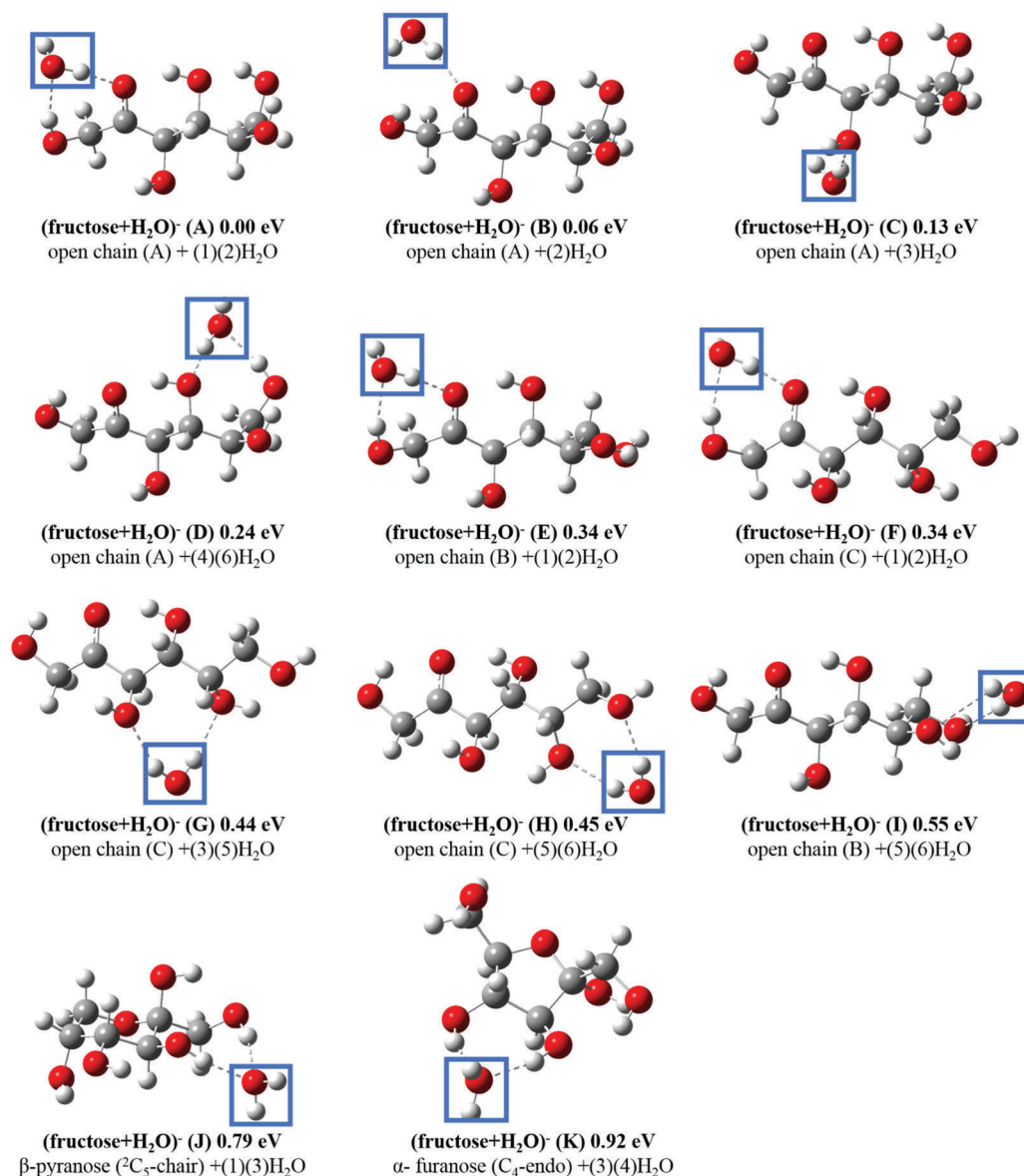
**Fig. 4** Optimized geometries of the typical low lying anionic isomers of (fructose + $H_2O$)$^-$ based on B3LYP/6-311++G(d,p) calculations. The relative energies and structural polymorphs are indicated. The blue squares indicate addition of an $H_2O$ unit at the marked position. The C ordering is the same as that of fructose$^-$ parent anions. For open chain structures (1)C to (6)C is ordered from left to right. For both furanose and pyranose structures (1)C to (6)C are ordered from right to left in a clockwise direction.

water–water hydrogen bonds. Its calculated VDE is 2.39 eV, also consistent with the experimental values. Isomer (fructose + $(H_2O)_3$)$^-$ (C) evolves from (fructose + $(H_2O)_2$)$^-$ (A) with the third water moiety only forming one water–water hydrogen bond. More isomers develop from (fructose + $(H_2O)_2$)$^-$ (A), (B) and (C) by adding the third $H_2O$ molecule at (2)O or (4)(5)(6)OH positions. They all have acceptable calculated VDEs consistent with the experimental determinations. Isomers (H) and (I) show water moieties residing parallel to the chain axis by forming water–water hydrogen bonds and water–fructose hydrogen bonds. Their theoretical VDEs (2.84 and 2.78 eV) are consistent with the experimental features. Isomers (K) and (L) have the identical added water moiety positions to (A), but with conformational

structure differences. They have comparable calculated VDEs to those observed. Isomer (fructose + $(H_2O)_3$)$^-$ (M) has a relative energy of 0.39 eV and evolves from (fructose + $(H_2O)_2$)$^-$ (K) with the third $H_2O$ moiety interacting with the carbonyl (2)O as well as forming a water–water hydrogen bond with the adjacent $H_2O$. Its theoretical VDE (2.51 eV) is also consistent with the experimental PES feature. Isomers (N) and (O) show pyranose geometry and isomers (P) and (Q) show furanose geometry. They have relative energies with respect to the lowest energy isomer of over 0.8 eV. Water molecules in these cyclic structures form a water–water hydrogen bond network that in turn interact with the bare fructose. They favor (1), (2), and (3) or (4)OH positions in the pyranose structure, and (3), (4)OH positions in the furanose
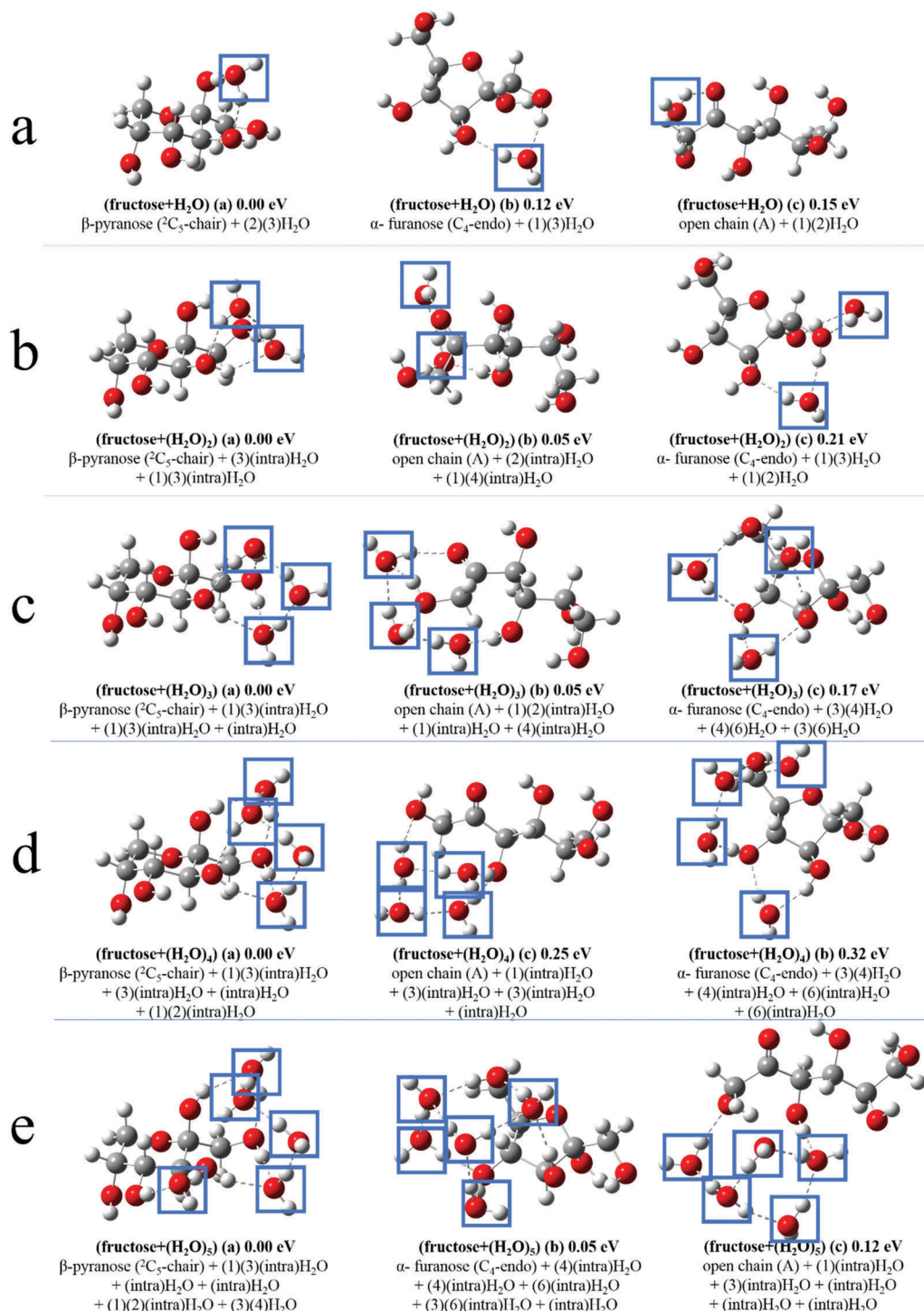
This journal is © the Owner Societies 2017

*Phys. Chem. Chem. Phys.*, 2017, **19**, 31121–31137 | **31127**

**Fig. 5** Optimized geometries of the lowest lying neutral isomers for open chain (A), pyranose, and furanose conformations of (fructose + $(H_2O)_n$) ($n$ = 1−2; a and b, respectively) based on B3LYP/6-311++G(d,p) and (fructose + $(H_2O)_n$) ($n$ = 3−5; c, d, and e, respectively) based on B3LYP/6-31++G(d) calculations. The relative energies and structural polymorphs are indicated. The blue squares indicate addition of $H_2O$ units at the marked position. The C ordering is the same as that of fructose⁻ parent anions. For open chain structures (1)C to (6)C is ordered from left to right. For both furanose and pyranose structures (1)C to (6)C is ordered from right to left in a clockwise direction.

structure. The calculated VDEs of these four cyclic isomers are 0.87–1.23 eV. These calculated VDE values are within the experimental PES low energy shoulder range from ∼0.5 to ∼1.5 eV. More cyclic structures can be found in the ESI.† Overall, the

broad photoelectron spectrum feature of (fructose + $(H_2O)_3$)⁻ is mostly dictated by positional and conformational open chain structures, for which water–water hydrogen bonds are most prevalent. Cyclic anions are also present in the experiment to
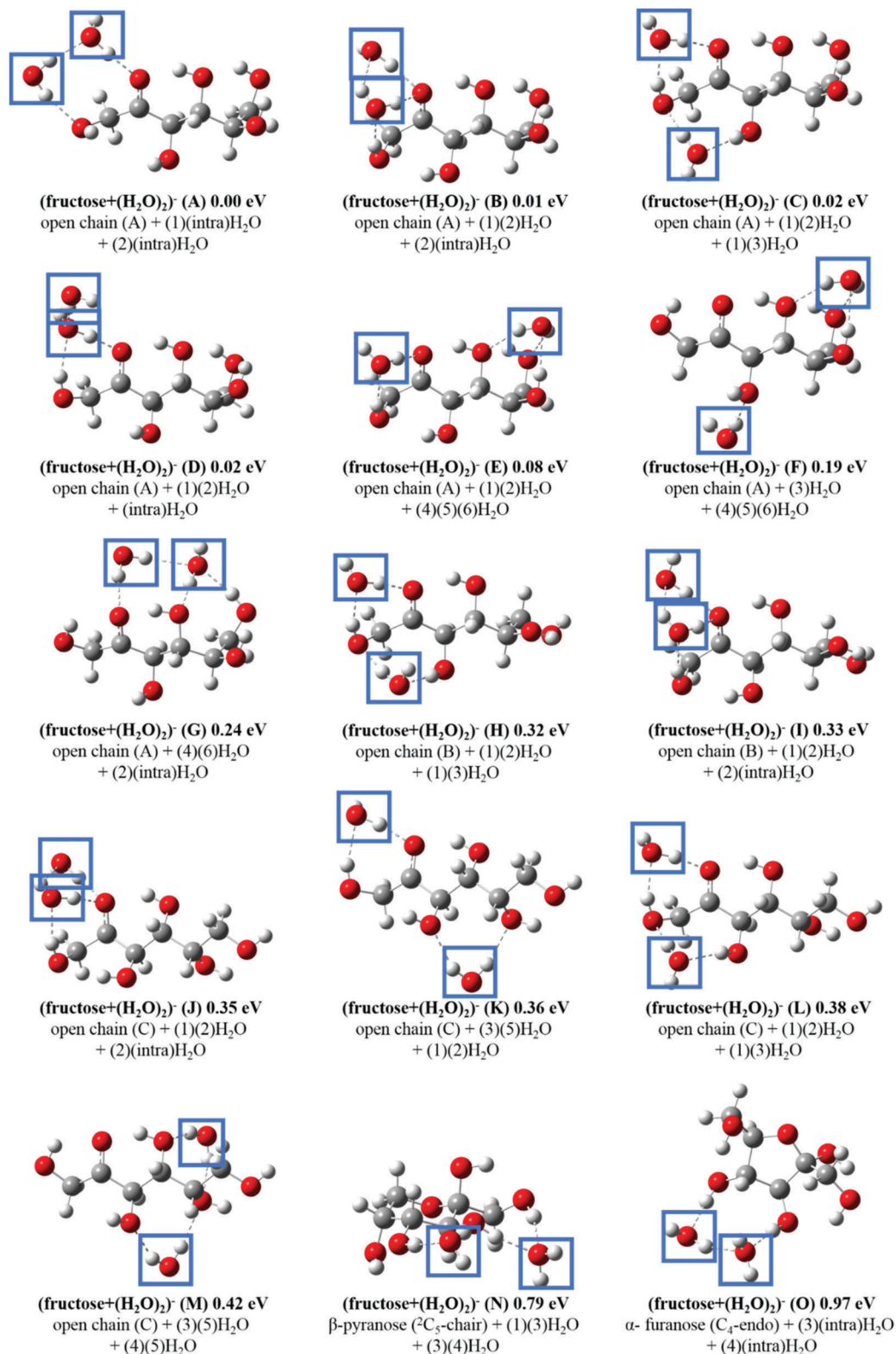
**31128** | *Phys. Chem. Chem. Phys.*, 2017, **19**, 31121–31137

This journal is © the Owner Societies 2017

**Fig. 6** Optimized geometries of the typical low lying anionic isomers of (fructose + $(H_2O)_2)^-$ based on B3LYP/6-311++G(d,p) calculations. The relative energies and structural polymorphs are indicated. The blue squares indicate addition of $H_2O$ units at the marked position. The C ordering is the same as that of fructose$^-$ parent anions. For open chain structures (1)C to (6)C is ordered from left to right. For both furanose and pyranose structures (1)C to (6)C is ordered from right to left in a clockwise direction.
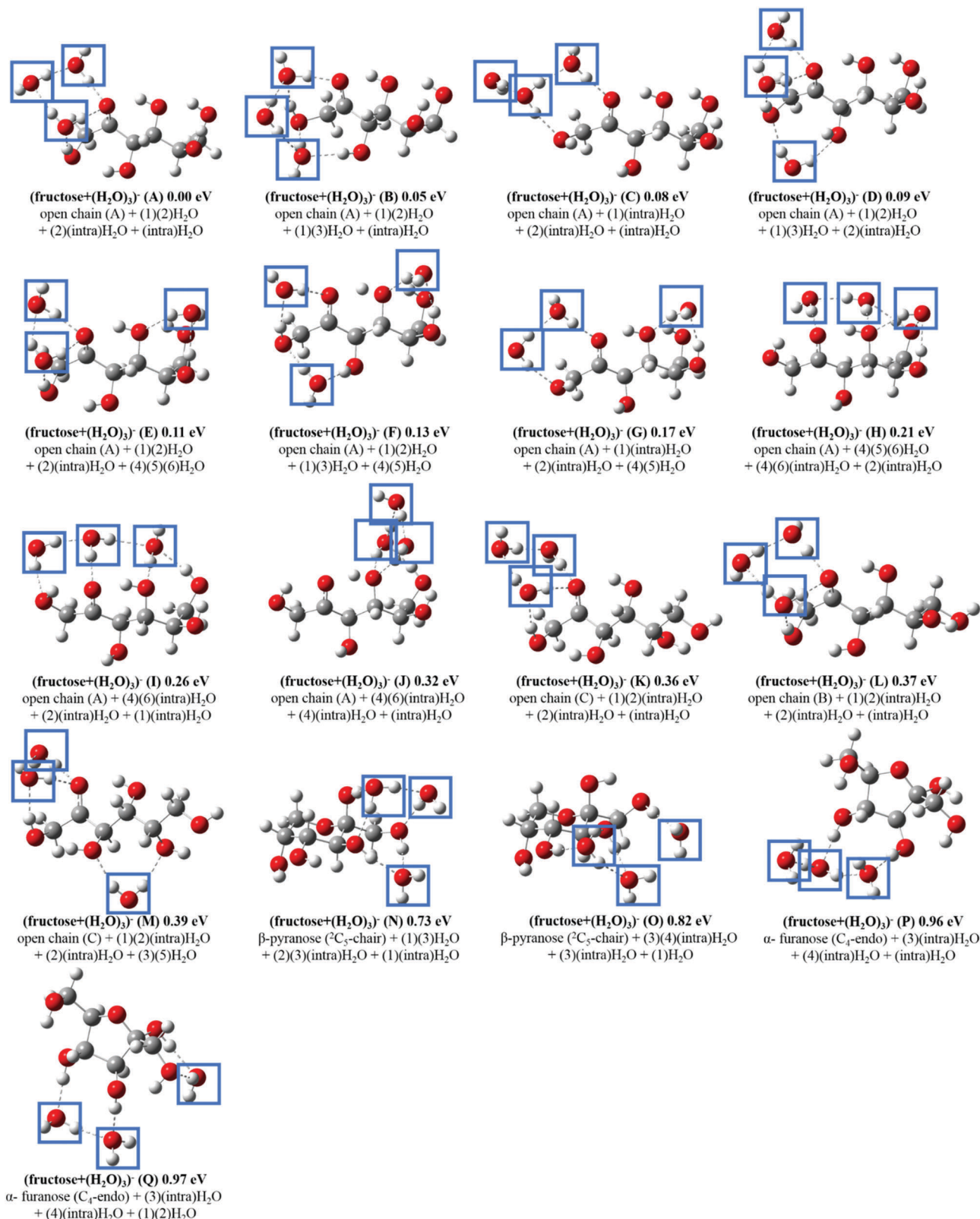
**(fructose+(H₂O)₃)⁻ (A) 0.00 eV**
open chain (A) + (1)(2)H₂O
+ (2)(intra)H₂O + (intra)H₂O

**(fructose+(H₂O)₃)⁻ (B) 0.05 eV**
open chain (A) + (1)(2)H₂O
+ (1)(3)H₂O + (intra)H₂O

**(fructose+(H₂O)₃)⁻ (C) 0.08 eV**
open chain (A) + (1)(intra)H₂O
+ (2)(intra)H₂O + (intra)H₂O

**(fructose+(H₂O)₃)⁻ (D) 0.09 eV**
open chain (A) + (1)(2)H₂O
+ (1)(3)H₂O + (2)(intra)H₂O

**(fructose+(H₂O)₃)⁻ (E) 0.11 eV**
open chain (A) + (1)(2)H₂O
+ (2)(intra)H₂O + (4)(5)(6)H₂O

**(fructose+(H₂O)₃)⁻ (F) 0.13 eV**
open chain (A) + (1)(2)H₂O
+ (1)(3)H₂O + (4)(5)H₂O

**(fructose+(H₂O)₃)⁻ (G) 0.17 eV**
open chain (A) + (1)(intra)H₂O
+ (2)(intra)H₂O + (4)(5)H₂O

**(fructose+(H₂O)₃)⁻ (H) 0.21 eV**
open chain (A) + (4)(5)(6)H₂O
+ (4)(6)(intra)H₂O + (2)(intra)H₂O

**(fructose+(H₂O)₃)⁻ (I) 0.26 eV**
open chain (A) + (4)(6)(intra)H₂O
+ (2)(intra)H₂O + (1)(intra)H₂O

**(fructose+(H₂O)₃)⁻ (J) 0.32 eV**
open chain (A) + (4)(6)(intra)H₂O
+ (4)(intra)H₂O + (intra)H₂O

**(fructose+(H₂O)₃)⁻ (K) 0.36 eV**
open chain (C) + (1)(2)(intra)H₂O
+ (2)(intra)H₂O + (intra)H₂O

**(fructose+(H₂O)₃)⁻ (L) 0.37 eV**
open chain (B) + (1)(2)(intra)H₂O
+ (2)(intra)H₂O + (intra)H₂O

**(fructose+(H₂O)₃)⁻ (M) 0.39 eV**
open chain (C) + (1)(2)(intra)H₂O
+ (2)(intra)H₂O + (3)(5)H₂O

**(fructose+(H₂O)₃)⁻ (N) 0.73 eV**
β-pyranose (²C₅-chair) + (1)(3)H₂O
+ (2)(3)(intra)H₂O + (1)(intra)H₂O

**(fructose+(H₂O)₃)⁻ (O) 0.82 eV**
β-pyranose (²C₅-chair) + (3)(4)(intra)H₂O
+ (3)(intra)H₂O + (1)H₂O

**(fructose+(H₂O)₃)⁻ (P) 0.96 eV**
α- furanose (C₄-endo) + (3)(intra)H₂O
+ (4)(intra)H₂O + (intra)H₂O

**(fructose+(H₂O)₃)⁻ (Q) 0.97 eV**
α- furanose (C₄-endo) + (3)(intra)H₂O
+ (4)(intra)H₂O + (1)(2)H₂O

**Fig. 7** Optimized geometries of the typical low lying anionic isomers of (fructose + (H₂O)₃)⁻ based on B3LYP/6-31++G(d) calculations. The relative energies and structural polymorphs are indicated. The blue squares indicate addition of H₂O units at the marked position. The C ordering is the same as that of fructose⁻ parent anions. For open chain structures (1)C to (6)C is ordered from left to right. For both furanose and pyranose structures (1)C to (6)C is ordered from right to left in a clockwise direction.
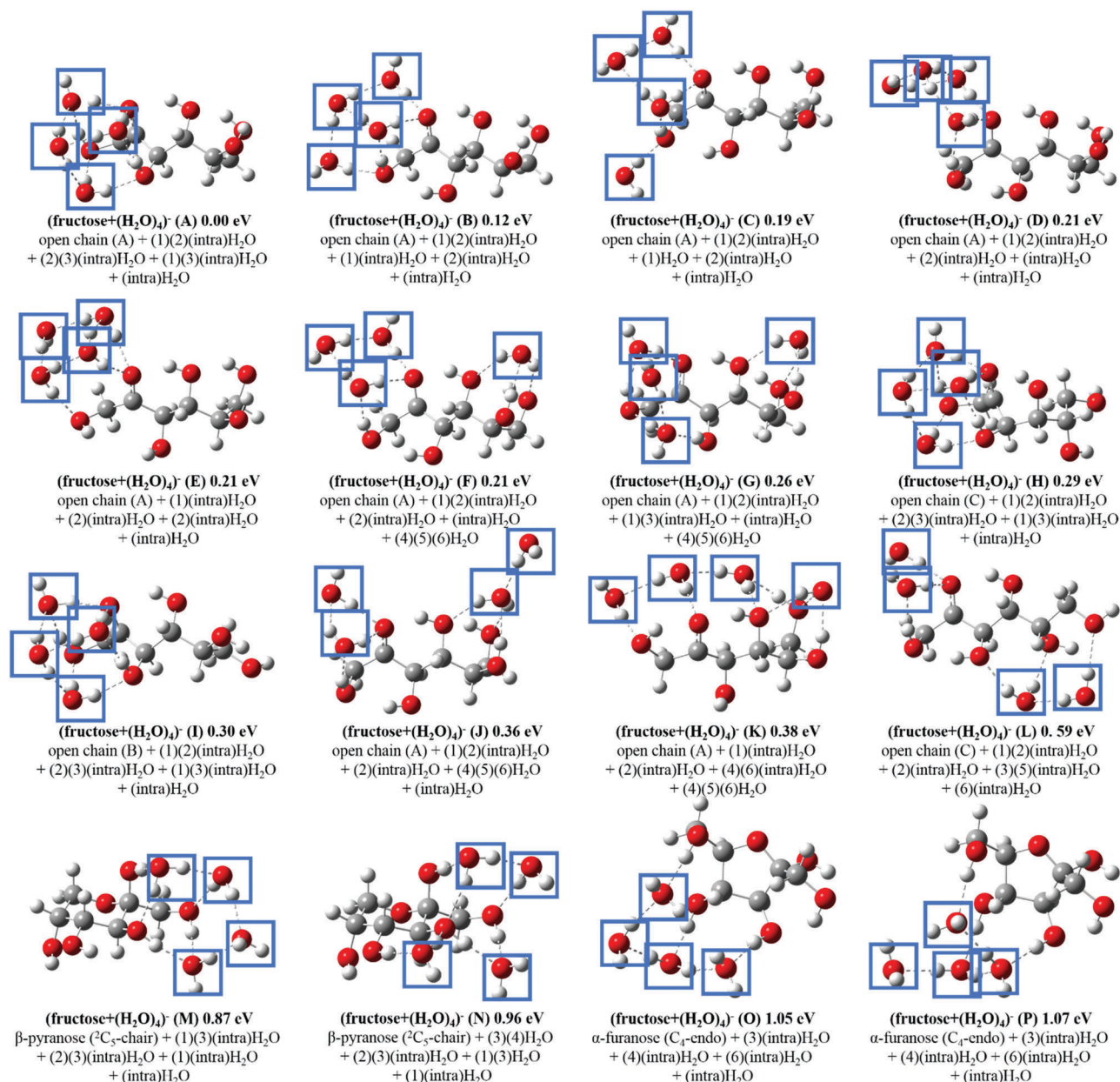
31130 | *Phys. Chem. Chem. Phys.,* 2017, **19**, 31121–31137

This journal is © the Owner Societies 2017

**Fig. 8** Optimized geometries of the typical low lying anionic isomers of (fructose + $(H_2O)_4)^-$ based on B3LYP/6-31++G(d) calculations. The relative energies and structural polymorphs are indicated. The blue squares indicate addition of $H_2O$ units at the marked position. The C ordering is the same as that of fructose$^-$ parent anions. For open chain structures (1)C to (6)C is ordered from left to right. For both furanose and pyranose structures (1)C to (6)C is ordered from right to left in a clockwise direction.

contribute to the PES feature shoulder. Fig. 5c shows that the lowest energy isomer of neutral (fructose + $(H_2O)_3$) clusters is still a pyranose one, as found for the smaller clusters. The molecules appear to form both water–water hydrogen bonds and water–fructose hydrogen bonds at (1) and (3) positions. The water moieties in neutral furanose conformation have interaction sites at (3), (4) and (6) positions, but without water–water hydrogen bond formation.

### d.   (Fructose + $(H_2O)_4)^-$

The typical low energy isomers of (fructose + $(H_2O)_4)^-$ are shown in Fig. 8. As can be anticipated, open chain isomers have lower

energy than cyclic anion isomers. Isomer (fructose + $(H_2O)_4)^-$ (A) can come from (fructose + $(H_2O)_3)^-$ (B) with the fourth $H_2O$ molecule binding to the carbonyl (2)O and the (3)OH group. The added water forms a water–water hydrogen bond with the third $H_2O$ molecule: this insertion generates a quasi-cubic structure at the (1)C side (including (1)OH, (2)O, and (3)OH) of fructose. The calculated VDE of isomer (A) is 2.88 eV, in good agreement with the experimental observation ($\sim$2.25 to $\sim$3 eV) of the broad PES feature. Isomer (fructose + $(H_2O)_4)^-$ (B) develops from (fructose + $(H_2O)_3)^-$ (A) by adding the fourth $H_2O$ molecule at the (1)OH position and forming a water–water hydrogen bond with the
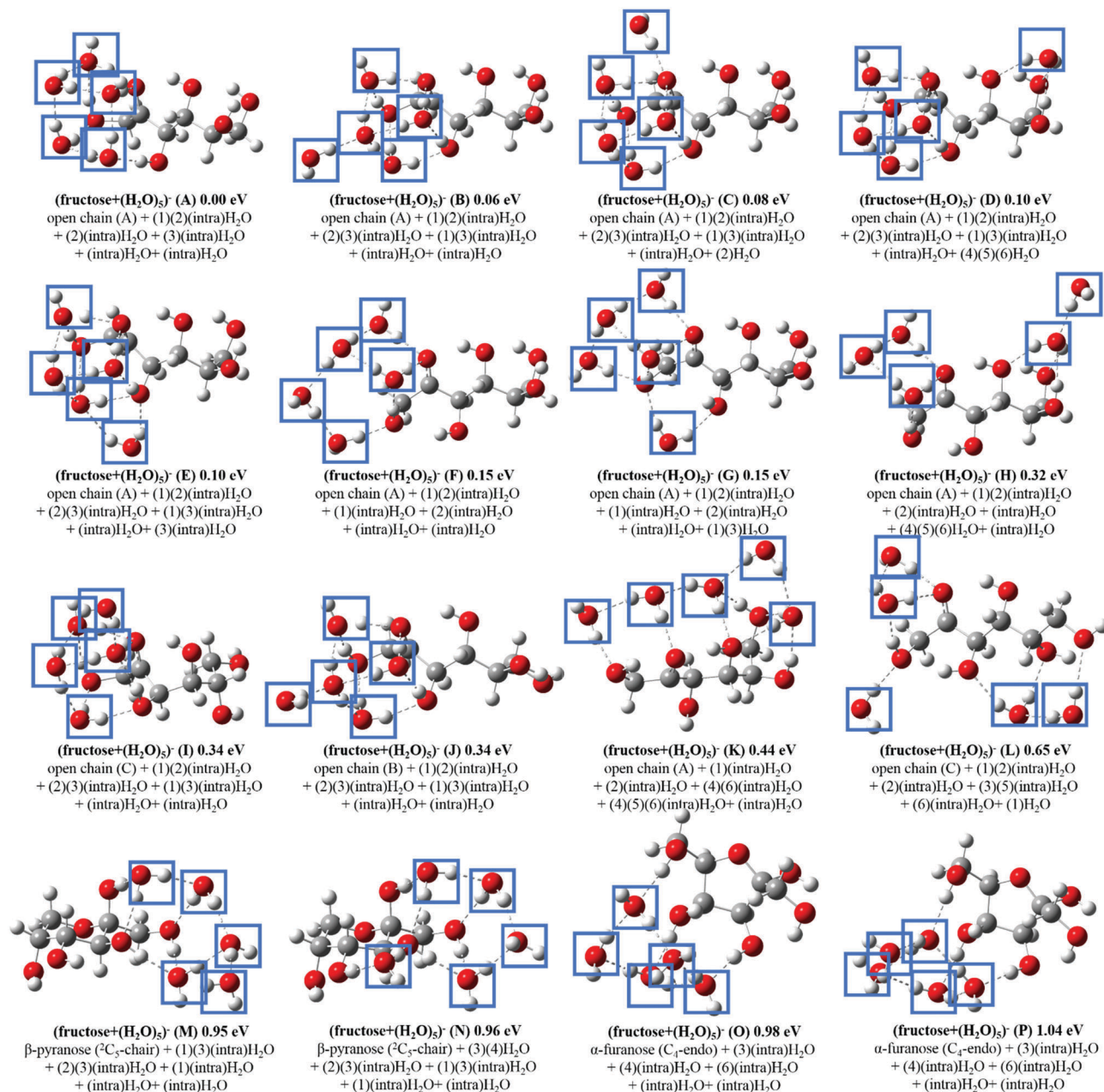
**Fig. 9** Optimized geometries of the typical low lying anionic isomers of (fructose + $(H_2O)_5$)$^-$ based on B3LYP/6-31++G(d) calculations. The relative energies and structural polymorphs are indicated. The blue squares indicate addition of $H_2O$ units at the marked position. The C ordering is the same as that of fructose$^-$ parent anions. For open chain structures (1)C to (6)C is ordered from left to right. For both furanose and pyranose structures (1)C to (6)C is ordered from right to left in a clockwise direction.

adjacent $H_2O$ molecule. Its theoretical VDE is 2.74 eV, consistent with the experimental values. Isomer (C) is similar to (B) but without the fourth $H_2O$ molecule forming a water–water hydrogen bond. It has a calculated VDE of 2.87 eV, in accord with the experimental results. Both isomers (D) and (F) also develop from (fructose + $(H_2O)_3$)$^-$ (A) by adding the fourth $H_2O$ molecule at different positions. Their calculated VDEs also match the experimental ones. Isomer (G) can be developed from the (fructose + $(H_2O)_3$)$^-$ (B) species with the fourth $H_2O$ interacting at (4), (5), and (6) OH positions. It has a calculated VDE of 2.62 eV,

in accord with the experimental determinations. Isomers (fructose + $(H_2O)_4$)$^-$ (E), (F), (J), (K), and (L) can evolve from (fructose + $(H_2O)_3$)$^-$ (A), (E), (E), (H), and (M), respectively. Their calculated VDEs all conform to the experimental estimations. Isomers (fructose + $(H_2O)_4$)$^-$ (H) and (I) have the similar quasi-cubic structure to isomer (A) but with conformational differences. Their calculated VDEs are 2.68 and 2.64 eV, respectively, also in agreement with the experimental determinations. Isomers (M) and (N) are pyranose related structures and both can develop from (fructose + $(H_2O)_3$)$^-$ (N) with the fourth $H_2O$

31132 | *Phys. Chem. Chem. Phys.*, 2017, **19**, 31121–31137

This journal is © the Owner Societies 2017

moiety forming two water–water hydrogen bonds in (M) and binding to (3)OH and (4)OH groups in (N). Their theoretical VDEs are 0.92 and 1.07 eV, respectively, in the range of the PES lower energy shoulder of (fructose + $(H_2O)_4)^-$. Both furanose isomers (fructose + $(H_2O)_4)^-$ (O) and (P) can come from (fructose + $(H_2O)_3)^-$ (P) with the fourth $H_2O$ molecule binding to (6)OH as well as forming a water–water hydrogen bond. They are conformationally distinct. The calculated VDEs (1.45 and 1.35 eV, respectively) of both isomers are consistent with the observed shoulder of the photoelectron feature for (fructose + $(H_2O)_4)^-$. Thus, the broad feature is mainly composed of many positional and conformational open chain isomers; cyclic isomer anions also exist in the experiment to contribute to the shoulder of the PES feature. As can be seen from Fig. 5d, the global minimum structure of neutral (fructose + $(H_2O)_4)^-$ is a pyranose one with water molecules binding to (1)OH, (2)OH, and (3)OH groups. The furanose structure has water moieties interacting with (3)OH, (4)OH, and (6)OH groups. The open chain isomer has a structure in which water molecules tend to form water clusters and interact with fewer OH groups of fructose compared to the corresponding anions.

### e. (Fructose + $(H_2O)_5)^-$

Fig. 9 shows the low energy isomers of (fructose + $(H_2O)_5)^-$, which also evidence the open chain isomers as the energetically favored conformations. The most stable isomer of (fructose + $(H_2O)_5)^-$ can evolve from (fructose + $(H_2O)_4)^-$ (A) by inserting the fifth water molecule between the (3)OH group and the adjacent water molecule. The theoretical VDE for this structure is 2.97 eV, in good agreement with the experimental determination ($\sim$2.88 to above $\sim$3.3 eV) from the broad PES feature. Isomers (fructose + $(H_2O)_5)^-$ (B), (C), (D), and (E) can also develop from (fructose + $(H_2O)_4)^-$ (A) by adding the fifth water molecule at different sites of the cubic $(H_2O)_4$ moiety structure or the fructose (4)(5)(6)OH groups. They have calculated VDEs (3.09, 3.22, 3.12, 3.14 eV, respectively): all these VDE values are consistent with the experimental observations. (Fructose + $(H_2O)_5)^-$ isomers (I) and (J) with a cubic structure and another water–water hydrogen bonded water moiety, arising from (fructose + $(H_2O)_4)^-$ (H) and (I), are conformationally different. Isomers (F) and (G) are from (fructose + $(H_2O)_4)^-$ (B) with the fifth water molecule interacting with the (1)OH group and the fourth water molecule or (1)(3)OH groups. The calculated VDEs of isomers (F) and (G) are 2.77 and 3.16 eV, respectively, also consistent with the experimental ones. Isomers (fructose + $(H_2O)_5)^-$ (H), (K), and (L) come from (fructose + $(H_2O)_4)^-$ (F), (K) and (L), respectively, with the fifth water molecule forming a water–water hydrogen bond or binding to the (1)OH group. Their calculated VDEs (2.98, 3.14, 2.94 eV) are also in accord with the experimental results. Anionic pyranose isomers (fructose + $(H_2O)_5)^-$ (M) and (N) can develop from (fructose + $(H_2O)_4)^-$ (M) with the fifth water molecule forming water–water hydrogen bonds. They have theoretical VDEs of 1.09 and 1.08 eV, respectively, and are outside the experimental feature width. Anionic fructose furanose isomers (fructose + $(H_2O)_5)^-$ (O) and (P) are from (fructose + $(H_2O)_4)^-$ (O) and (P) with the fifth water

molecule forming water–water hydrogen bonds. Their calculated VDEs (1.38 and 1.43 eV, respectively) are also lower than the experimental estimations. Overall, the photoelectron spectrum of (fructose + $(H_2O)_5)^-$ is contributed by open chain isomers with positional and conformational differences. As shown in Fig. 5e, the neutral (fructose + $(H_2O)_5$) cluster also appears to have a pyranose geometry as the most stable structure. The fifth water molecule binds to (3)OH and (4)OH groups. For both neutral furanose and open chain isomers, the fifth water molecules only form water–water hydrogen bonds.

## VI. Discussion

Based on the good agreement between experimental and theoretical VDEs, as well as the consistent calculated VDEs from different DFT computational functionals, the anionic structures of (fructose + $(H_2O)_n)^-$ ($n$ = 1–5) are validated and assigned. Neutral structures are also provided by employing the experimentally validated calculation algorithm. (Fructose + $(H_2O)_n)^-$ ($n$ = 1–5) mainly exist in the present experiments as open chain structures. Some cyclic anions of (fructose + $(H_2O)_n)^-$ ($n$ = 3–4) are also present in the experiments. Many positional and conformational open chain isomers coexist to contribute to the broad PES features of (fructose + $(H_2O)_n)^-$ ($n$ = 1–5). Open chain anionic isomers have much lower energy than cyclic anionic geometries for every specific cluster.

For open chain anionic isomers, the first water molecule can interact with every OH groups or carbonyl O of fructose as an acceptor or donor in a hydrogen bond. At $n$ = 2, water molecules can interact with fructose separately or bind to it through a water dimer. With $n$ = 3 to 5, water moieties form water–water hydrogen bonds and bind to fructose. A quasi-cubic structure at the end of the (1)C side (including (1)OH, (2)O, and (3)OH) of fructose starts to form as the most stable structure for (fructose + $(H_2O)_4)^-$ and continues to appear as the lowest energy isomers of (fructose + $(H_2O)_5)^-$. This suggests that water–fructose hydrogen bond strength for the open chain anion is comparable to that of a water–water hydrogen bond. A second hydration shell of open chain fructose$^-$ can form at $n$ = 3. The binding sites on fructose can act both as a donor and an acceptor in the hydrogen bond interaction with water molecules.

Cyclic anions have much lower VDEs than those of open chain ones. With increasing number of water molecules, the VDEs increase from $\sim$0.40 eV in (fructose + $H_2O)^-$ to $\sim$1.38 eV in (fructose + $(H_2O)_5)^-$. Water molecules associated with a pyranose conformer bind preferentially with (1)OH, (2)OH, and (3)OH groups, and bind to (3)OH, (4)OH, and (6)OH sites associated with a furanose conformer. The interaction sites in pyranose are both donors and acceptors, while the OH groups of furanose conformations interact with water as donors. A second hydration shell can be formed at $n$ = 4 and $n$ = 3 in pyranose and furanose conformations, respectively.

In order to understand the observed (fructose + $(H_2O)_n)^-$ ($n$ = 1–5) behavior from the view point of electronic structure, a Natural Bond Orbital (NBO) analysis is performed based on

This journal is © the Owner Societies 2017

*Phys. Chem. Chem. Phys.*, 2017, **19**, 31121–31137 | 31133

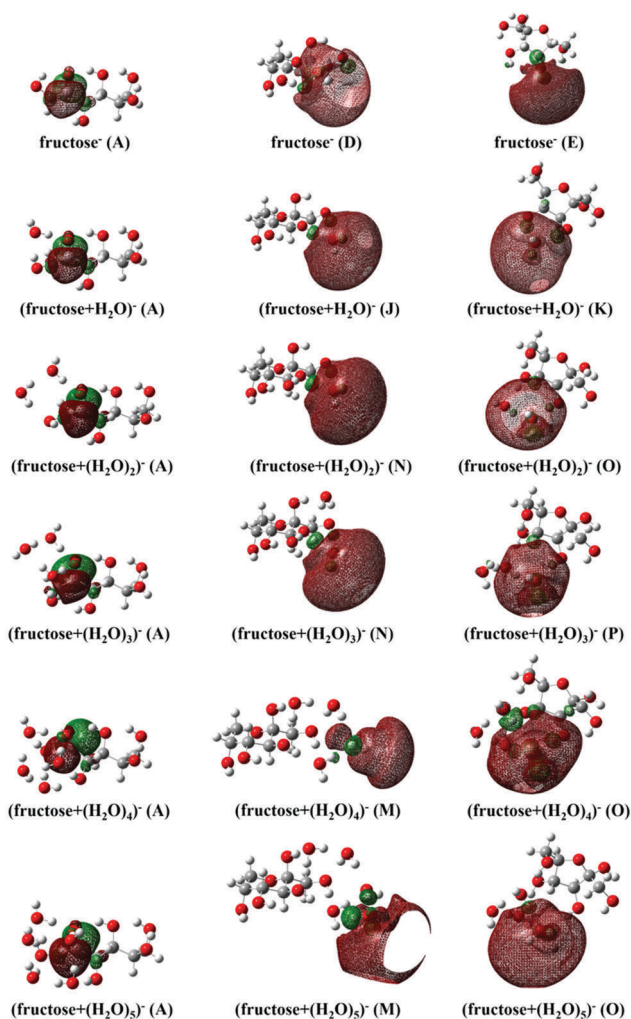**Fig. 10** NBO/HOMOs (highest occupied molecular orbitals) of the lowest energy open chain (A), pyranose, and furanose structures of (fructose + $(H_2O)_n)^-$ ($n = 0–2$) anions from an NBO analysis based on B3LYP/6-311++G(d,p) and (fructose + $(H_2O)_n)^-$ ($n = 3–5$) anions based on B3LYP/6-31++G(d) calculations. Open chain structures of (fructose + $(H_2O)_n)^-$ ($n = 0–5$) anions all show valence bound extra electron wave functions mostly localized on (2)C p orbitals, while cyclic structures display dipole bound character with the added electron transferring from parent anion to water molecules with increased numbers of water molecules.

the B3LYP/6-311++G(d,p) or B3LYP/6-31++G(d) level of theory. The molecular orbitals of the lowest energy open chain (A), pyranose, and furanose structures of (fructose + $(H_2O)_n)^-$ ($n = 0–5$), generated from an NBO analysis, are presented in Fig. 10.

The NBO/HSOMO (highest singly occupied molecular orbital) of the most stable open chain (A) anion displays a valence bound anion electronic distribution mainly located in a p orbital of (2)C in both fructose$^-$ bare ions and (fructose + $(H_2O)_n)^-$ ($n = 1–5$) anionic clusters. The NBO/HSOMOs of the most stable pyranose and furanose anions show diffuse dipole-bound states in both a fructose$^-$ bare ion and (fructose + $(H_2O)_n)^-$ ($n = 1–5$): the excess electron eventually transfers from the dangling H of the OH groups of the parent cyclic anions to the water molecules. The excess electron wave function further illustrates that open

chain structures are more stable than cyclic structures for the (fructose + $(H_2O)_n)^-$ ($n = 1–5$) anionic clusters. The water molecules in the cyclic conformations stabilize the cyclic structures by increasing the excess electron binding ability via increased dipole moment from an average of $\sim 4.4$ D for the bare ion to $\sim 7.3$ D at $n = 5$.

Neutral (fructose + $(H_2O)_n$) ($n = 1–5$) clusters have pyranose conformations as the global minimum structures rather than open chain or furanose conformations. This is consistent with solution phase results, for which β-fructopyranose is the major tautomer. The water moieties constitute water–water hydrogen bond networks, and bind to (1)OH, (2)OH, and (3)OH groups in neutral pyranose conformations. For larger neutral furanose structures (fructose + $(H_2O)_n$) ($n = 3–5$), the water molecules also interact with (3)OH, (4)OH, and (6)OH sites, similar to those found for the corresponding anions. In the neutral open chain conformations, water molecules mostly interact with fewer OH sites of fructose than do the corresponding anions. A second hydration shell starts to form at $n = 3$, $n = 5$, and $n = 4$ for neutral pyranose, furanose, and open chain conformations, respectively. The interaction sites of the three kinds of neutral conformations act as both donors and acceptors.

From our previous paper,[37] fragmentation ions (fructose–X)$^-$ (X = H, OH, H$_2$O) can be observed and are accessed as the characteristic fragmentation ions of the parent fructose species. Recall that many isomers of the (fructose–H)$^-$ anion coexist in the gas phase, including open chain and pyranose structures. (Fructose–OH)$^-$ mainly coexist as open chain structures. (Fructose–H$_2$O)$^-$ is present in these samples as two kinds of positional isomers, one from a furanose ring opening structure, and the other from an open chain structure. In the present study, (fructose + $(H_2O)_n)^-$ ($n = 1–5$) anions mainly exist as open chain structures, while neutral (fructose + $(H_2O)_n$) ($n = 1–5$) clusters have pyranose conformations as the global minimum structures rather than open chain or furanose conformations. Thus, the data strongly suggest that a total neutral and/or anion cascade fragmentation to small, few atomic species does not occur for fructose and its related isomers, with and without solvation by water. Additionally, no such small molecule species are readily observable in the TOFM spectra.

Monosaccharides are flexible polymorphic species, presenting a collection of rich and complex constitutional, configurational, and conformational isomers. When monosaccharides are hydrated, even more isomeric forms can be expected to appear. Since this is the first spectroscopic study (PES or other) of any of these samples and species, the reported data are unique, and in conjunction with the calculations, such isomeric behavior is well documented and demonstrated. If the spectra were sharp and well resolved, the species would have a single lowest energy form that would be identified by its well resolved VDE. Such big and flexible molecules usually have broad overlapping vibrational and rotational excitations, which also induce broad features in vibrational spectra as found for most solvated clusters even of rigid molecules. Our PES experiments coupled with DFT calculations can provide a full landscape for structural characterization of monosaccharide neutrals and anions, as well

as their microhydrated species. These findings can be precedents for further structural characterization of specific isomers using other spectroscopic techniques. Our study also provides general conclusions concerning preferred interaction sites for fructose pyranose, furanose, and open chain conformations with water molecules. These data present the form of the potential energy surfaces for both the isolated and solvated, neutral and anionic species accessed. This information provides insight into the elucidation of microhydrated fructose. For every specific isomer, molecular dynamics simulations of the hydration process can be performed that might reveal the structural dynamics of the local minima these results have uncovered. Such dynamical studies are beyond the scope of the present report because the experimental results refer only to the potential minima we have presented and not the full (barriers and transition states) along the multifaceted reaction coordinates connecting these minima.

In order to draw comparisons between the behavior of different monosaccharides with regard to cluster formation with, and solvation by water, microscopic hydration studies of ribose are currently underway in our laboratory employing the same techniques reported herein. Ribose + $H_2O_{1,2\ldots}^-$ cluster anions are, however, not observed in the TOFM spectrum. Recall that the ribose parent anion is not observed in the present experiments, but the fructose parent anion is, implying that the ribose parent anion is not as stable a species as the fructose parent anion. Thus, ribose + $H_2O_{1,2\ldots}^-$ clusters might not be expected to exist in the present experiments, based on the low concentration of its parent anion. Such absence can also possibly be understood from the point of view of the solubility of the different monosaccharides in water. Fructose (a ketohexose) has a very high solubility in water ($>3 \times 10^3$ g L$^{-1}$@25 °C), while the solubility of ribose (an aldopentose) in water is comparatively relatively quite low ($\sim 100$ g L$^{-1}$@25 °C) for any monosaccharide. The absence of ribose + $H_2O_{1,2\ldots}^-$ cluster anions, but the presence of fructose + $H_2O_{1,2\ldots}^-$ cluster anions, implies a stronger interaction between fructose and water than between ribose and water. Such behavior is consistent with both the presently reported cluster and solubility data.

More pentose (*e.g.*, arabinose, ribulose...) and hexose (*e.g.*, mannose, talose, tagatose...) aldo/keto-monosaccharides will be explored both experimentally and theoretically to compare comprehensively and systematically these uncovered behavioral differences. The choices of different monosaccharides are discussed in detail in the ESI.†

# VII. Conclusions

We execute anion photoelectron spectroscopic studies coupled with density functional theory based calculations for (fructose + $(H_2O)_n)^-$ ($n = 1$–5) clusters to reveal the microscopic hydration processes for fructose in water, as well as the interaction (binding) sites of fructose with other molecules. The vertical detachment energies of anionic clusters are experimentally determined and their anionic structures are assigned based on good agreement between experimental and theoretical vertical detachment energies. Both conformational and positional isomers are considered and assigned. Conformational isomers (open chain, furanose, pyranose,...) have different geometries, but the same positions for added $H_2O$ moieties. Positional isomers have different added $H_2O$ moiety positions, but similar conformations. The corresponding neutral structures are also calculated employing the experimentally validated calculation algorithm.

Gas phase, isolated (fructose + $(H_2O)_n)^-$ ($n = 1$–5) clusters mainly exist as open chain structures in the presented experiments. Many conformational and positional isomers coexist to contribute to the broad PES features of (fructose + $(H_2O)_n)^-$ ($n = 1$–5). For small (fructose + $(H_2O)_n)^-$ ($n = 1$–2) clusters, water molecules can interact with fructose$^-$ separately or bind to it through water dimer clusters. With increasing numbers of bound water molecules, water molecules form water–water hydrogen bonds, as well as bind to fructose. Water molecules interact with the (1)C side (including (1)OH, (2)O, and (3)OH) of fructose$^-$ and finally form a quasi-cubic structure with OH groups and carbonyl O in the most stable structures for (fructose + $(H_2O)_4)^-$ and (fructose + $(H_2O)_5)^-$.

Cyclic structures (pyranose and furanose) of (fructose + $(H_2O)_n)^-$ ($n = 1$–5) anions have much higher energies than the lowest energy open chain isomers, and smaller VDEs than those for open chain structures. With increasing number of water molecules, the VDEs of cyclic structures increase gradually from $\sim 0.40$ eV in (fructose + $H_2O)^-$ to $\sim 1.38$ eV in (fructose + $(H_2O)_5)^-$. Cyclic fructose$^-$ and cyclic (fructose + $(H_2O)_n)^-$ ($n = 1$–5) have the added electron as dipole bound, whereas the open chain structures (fructose + $(H_2O)_n)^-$ ($n = 0$–5) have the added electron in a valence orbital. Water molecules stabilize the cyclic anions. Cyclic structures of (fructose + $(H_2O)_n)^-$ ($n = 3$, 4) are apparently present in the experiments and their VDEs can contribute to the shoulders of PES features for (fructose + $(H_2O)_n)^-$ ($n = 3$, 4). Water molecules solvating cyclic anions form water–water hydrogen bond networks that interact with OH groups of fructose$^-$: OH groups at (1), (2), and (3) positions of fructose pyranose anions, and (3), (4), and (6) positions at fructose furanose anions are most active in this solvation. A second hydration shell can form at $n = 3$ for open chain anionic geometries, and at $n = 4$ and $n = 3$ for pyranose and furanose anionic conformations, respectively.

Neutral structures of (fructose + $(H_2O)_n)$ ($n = 1$–5) have pyranose structures as the lower energy isomers rather than open chain structures, consistent with the fructose solution tautomeric equilibrium with the fructose pyranose species being the preponderant one. Similar to anionic structures, water molecules tend to form water–water hydrogen bond networks and interact with OH groups at (1), (2), and (3) positions for neutral pyranose conformations. For larger furanose (fructose + $(H_2O)_n)$ ($n = 3$–5) clusters, water molecules bind to OH groups at (3), (4), and (6) positions. Solvation of open chain neutral fructose occurs mostly through water clusters, which interact with fewer OH sites of fructose than do the corresponding anions. A second hydration shell starts to form at $n = 3$, $n = 5$, and $n = 4$ for pyranose, furanose, and open chain neutral conformations, respectively.

This journal is © the Owner Societies 2017

*Phys. Chem. Chem. Phys.*, 2017, **19**, 31121–31137 | **31135**

The OH groups of fructose in pyranose and open chain conformations interact with water as both donor and acceptor sites in hydrogen bonding interactions for both anions and neutrals. The OH groups of furanose conformations interact with water as donors in anions, while in neutrals, they interact as both donor and acceptor sites.

Structures of water–saccharide solvation at the atomistic level, based on an NBO analysis, can enhance the understanding of the functional behavior of fructose as it binds to receptors in biological systems. For example, the degree of sweetness associated with sugar–receptor interactions, and the relation between the sugar structure, solvation, and sweetness are both specific solvation site dependent and degree of solvation dependent.

## Conflicts of interest

There are no conflicts of interest to declare.

## Acknowledgements

## References

1 F. A. Quiocho, D. K. Wilson and N. K. Vyas, *Nature*, 1989, **340**, 404.

2 C. Clarke, R. J. Woods, J. Gluska, A. Cooper, M. A. Nutley and G.-J. Boons, *J. Am. Chem. Soc.*, 2001, **123**, 12238.

3 A. Ben-Naim, *Biophys. Chem.*, 2002, **101**, 309.

4 C. A. Bottoms, P. E. Smith and J. J. Tanner, *Protein Sci.*, 2002, **11**, 2125.

5 M. Cockman, D. G. Kubler, A. S. Oswald and L. Wilson, *J. Carbohydr. Chem.*, 1987, **6**, 181.

6 V. A. Yaylayan, A. A. Ismail and S. Mandeville, *Carbohydr. Res.*, 1993, **248**, 355.

7 T. L. Mega, S. Cortes and R. L. Van Etten, *J. Org. Chem.*, 1990, **55**, 522.

8 W. Funcke, C. von Sonntag and C. Triantaphylides, *Carbohydr. Res.*, 1979, **75**, 305.

9 T. Barclay, M. Ginic-Markovic, M. R. Johnston, P. Cooper and N. Petrovsky, *Carbohydr. Res.*, 2012, **347**, 136.

10 P. Çarçabal, R. A. Jockusch, I. Hünig, L. C. Snoek, R. T. Kroemer, B. G. Davis, D. P. Gamblin, I. Compagnon, J. Oomens and J. P. Simons, *J. Am. Chem. Soc.*, 2005, **127**, 11414.

11 M. T. I. Mredha, C. K. Roy, M. M. Rahman, M. Y. A. Mollah and M. A. B. H. Susan, *Electrochim. Acta*, 2013, **97**, 231.

12 T. Afrin, N. N. Mafy, M. M. Rahman, M. Y. A. Mollah and M. A. B. H. Susan, *RSC Adv.*, 2014, **4**, 50906.

13 J.-J. Max and C. Chapados, *J. Phys. Chem. A*, 2007, **111**, 2679.

14 C. Branca, S. Magazù, G. Maisano and P. Migliardo, *J. Chem. Phys.*, 1999, **111**, 281.

15 A. Lerbret, P. Bordat, F. Affouard, Y. Guinet, A. Hédoux, L. Paccou, D. Prévost and M. Descamps, *Carbohydr. Res.*, 2005, **340**, 881.

16 K. Shiraga, T. Suzuki, N. Kondo, J. De Baerdemaeker and Y. Ogawa, *Carbohydr. Res.*, 2015, **406**, 46.

17 L. R. Winther, J. Qvist and B. Halle, *J. Phys. Chem. B*, 2012, **116**, 9196.

18 C. Branca, S. Magazù, F. Migliardo and P. Migliardo, *Physica A*, 2002, **304**, 314.

19 C. Branca, S. Magazù, G. Maisano, F. Migliardo, P. Migliardo and G. Romeo, *J. Phys. Chem. B*, 2001, **105**, 10140.

20 K. Shiraga, A. Adachi, M. Nakamura, T. Tajima, K. Ajito and Y. Ogawa, *J. Chem. Phys.*, 2017, **146**, 105102.

21 S. L. Lee, P. G. Debenedetti and J. R. Errington, *J. Chem. Phys.*, 2005, **122**, 204511.

22 A. Lerbret, P. Bordat, F. Affouard, M. Descamps and F. Migliardo, *J. Phys. Chem. B*, 2005, **109**, 11046.

23 M. T. Sonoda and M. S. Skaf, *J. Phys. Chem. B*, 2007, **111**, 11948.

24 M. H. H. Pomata, M. T. Sonoda, M. S. Skaf and M. D. Elola, *J. Phys. Chem. B*, 2009, **113**, 12999.

25 R. S. Shallenberger and T. E. Acree, *Nature*, 1967, **216**, 480.

26 R. S. Shallenberger, T. E. Acree and W. E. Guild, *J. Food Sci.*, 1965, **30**, 560.

27 L. B. Kier, *J. Pharm. Sci.*, 1972, **61**, 1394.

28 A. van der Heijden, L. B. P. Brussel and H. G. Peer, *Food Chem.*, 1978, **3**, 207.

29 R. S. Shallenberger and M. G. Lindley, *Food Chem.*, 1977, **2**, 145.

30 T. Yamazaki, E. Benedetti, D. Kent and M. Goodman, *Angew. Chem., Int. Ed. Engl.*, 1994, **33**, 1437.

31 C. Nofre and J.-M. Tinti, *Food Chem.*, 1996, **56**, 263.

32 M. Mathlouthi, *Food Chem.*, 1984, **13**, 1.

33 N. H. Rhys, F. Bruni, S. Imberti, S. E. McLain and M. A. Ricci, *J. Phys. Chem. B*, 2017, **121**, 7771.

34 H.-S. Im and E. R. Bernstein, *J. Chem. Phys.*, 2000, **113**, 7911.

35 S. Yin and E. R. Bernstein, *J. Chem. Phys.*, 2016, **145**, 154302.

36 B. Yuan, Z. Yu and E. R. Bernstein, *J. Chem. Phys.*, 2015, **142**, 124315.

37 Z. Zeng and E. R. Bernstein, *Phys. Chem. Chem. Phys.*, 2017, **19**, 23325.

38 Z. Zeng and E. R. Bernstein, *Phys. Chem. Chem. Phys.*, 2017, **19**, 28950.

39 A. D. Becke, *J. Chem. Phys.*, 1993, **98**, 5648.

40 C. Lee, W. Yang and R. G. Parr, *Phys. Rev. B: Condens. Matter Mater. Phys.*, 1988, **37**, 785.

41 A. D. Becke, *Phys. Rev. A: At., Mol., Opt. Phys.*, 1988, **38**, 3098.

42 M. J. Frisch, G. W. Trucks, H. B. Schlegel, G. E. Scuseria, M. A. Robb, J. R. Cheeseman, G. Scalmani, V. Barone, B. Mennucci, G. A. Petersson, H. Nakatsuji, M. Caricato, X. Li, H. P. Hratchian, A. F. Izmaylov, J. Bloino, G. Zheng, J. L. Sonnenberg, M. Hada, M. Ehara, K. Toyota, R. Fukuda, J. Hasegawa, M. Ishida, T. Nakajima, Y. Honda, O. Kitao,

31136 | *Phys. Chem. Chem. Phys.*, 2017, **19**, 31121–31137

This journal is © the Owner Societies 2017

H. Nakai, T. Vreven, J. A. M. Jr., J. E. Peralta, F. Ogliaro, M. Bearpark, J. J. Heyd, E. Brothers, K. N. Kudin, V. N. Staroverov, R. Kobayashi, J. Normand, K. Raghavachari, A. Rendell, J. C. Burant, S. S. Iyengar, J. Tomasi, M. Cossi, N. Rega, J. M. Millam, M. Klene, J. E. Knox, J. B. Cross, V. Bakken, C. Adamo, J. Jaramillo, R. Gomperts, R. E. Stratmann, O. Yazyev, A. J. Austin, R. Cammi, C. Pomelli, J. W. Ochterski, R. L. Martin, K. Morokuma, V. G. Zakrzewski, G. A. Voth, P. Salvador, J. J. Dannenberg, S. Dapprich, A. D. Daniels, O. Farkas, J. B. Foresman, J. V. Ortiz, J. Cioslowski and D. J. Fox, *Gaussian 09, Revision A.02*, Gaussian, Inc., Wallingford, CT, 2009.

43 Y. Zhao and D. G. Truhlar, *Theor. Chem. Acc.*, 2008, **120**, 215.

44 Y. Zhao and D. G. Truhlar, *Acc. Chem. Res.*, 2008, **41**, 157.